Appl. Phys. B 44, 125–132 (1987)

Applied Physics B Photophysics and Laser Chemistry

Longitudinal Resonant Spectrophone for CO-Laser Photoacoustic Spectroscopy

S. Bernegger and M. W. Sigrist

Institute of Quantum Electronics, Physics Department, ETH, Hoenggerberg, CH-8093 Zürich, Switzerland

Received 16 February 1987/Accepted 30 April 1987

Abstract. A photoacoustic (PA) system for monitoring gaseous air pollutants absorbing in the CO-laser range is presented. The characteristics of the CO laser and the interference caused by water-vapor absorption demand a special design of the PA cell and experimental setup. The optimum cell design was found by numerical simulation of the acoustic properties of various cell geometries. For this purpose a model using infinitesimal analogue acoustic impedances was developed. Based on a matrix formalism for four-terminals, a computer program was applied that permits the calculation of the frequency response of the PA signal amplitude at any position within a one-dimensional PA cell. Excellent agreement with experimental data is obtained. As a result, a new design for an acoustically resonant spectrophone with improved properties is presented. The response of the cell with a Q-factor of 52, operated at 555 Hz, is 2000 Pa cm/W.

PACS: 07.65b, 43.20f, 43.85e

Photoacoustic spectroscopy (PAS) with tunable infrared lasers as a source of radiation has been shown to be a very suitable instrument for monitoring gaseous air pollutants at low concentrations [1–3]. Many important molecules like nitric oxide (NO), nitrogen dioxide (NO_2), ethylene (C_2H_4), propylene (C_3H_6), 1,3-butadiene (C_4H_6), formaldehyde (H_2CO), ammonia (NH_3) etc., show strong absorption bands between 5.0 and 6.5 μm. Therefore, a CO laser which can be tuned over approximately 90 lines with output powers between 5 mW and 1 W within this wavelength range is of special interest as a source of radiation [4].

However, a severe problem for CO-laser PAS of air samples is caused by the interference of water vapor absorption. If trace gas concentrations in the ppbv range should be detected, a precise correction of the measured PA spectrum of the air sample with respect to the water vapor absorption is necessary. This correction is rent more difficult by the special features of the CO laser which usually emits couples or even triples of close laser lines simultaneously [5].

1. CO-Laser-Photoacoustic Spectroscopy of Gases

1.1. Water-Vapor Absorption of CO-*Laser Radiation*

The effect of multiple emission of the CO laser is shown in Fig. 1 where the laser power is plotted versus the wavenumber which is derived from the grating angle. The position of the CO-laser lines $P(10)$–$P(28)$ of the vibrational transitions 4–3 up to 22–21 are marked with ticks. Even if the position of the maximum of some lines differs slightly from the predicted position because of mechanical fluctuations caused by the grating-drive mechanism, most transitions can be identified. It is easy to recognize that in general at least two lines are emitted simultaneously. These lines are separated by up to 1 cm^{-1} and are not resolved by the CO-laser grating (150 lines/mm, blazed at 6.0 μm).

The absorption cross sections of small molecules like H_2O can differ appreciably for adjacent CO-laser lines. This is illustrated in Table I where H_2O-vapor absorption cross sections calculated on the basis of AFGL data are listed [6]. The measured absorption

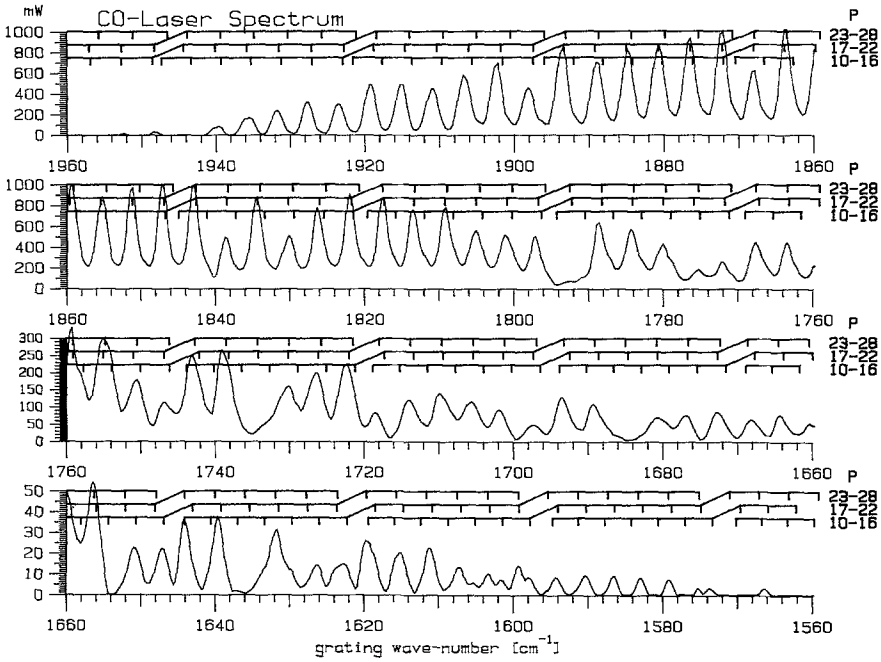

Fig. 1. Output power of the $^{12}C^{16}O$-laser versus wavenumber of the grating. The ticks represent the vibrational-rotational *P* transitions of the CO molecule

Table I. Calculated absorption cross sections of water vapor for selected CO-laser lines

CO-Laser Line		H_2O Absorption Cross Section
Transition	[cm^{-1}]	[$10^{-21} cm^2$/Molecule]
5- 4 P(28)	1921.320	0.283
6- 5 P(22)	1922.983	7.459
7- 6 P(16)	1923.154	47.406
9- 8 P(23)	1842.821	1.285
10- 9 P(17)	1842.816	1.278
11-10 P(11)	1841.300	0.368
9- 8 P(27)	1825.316	85.267
10- 9 P(21)	1826.214	1.295
11-10 P(15)	1825.621	6.952
11-10 P(23)	1792.699	299.669
12-11 P(17)	1792.433	45.411
13-12 P(11)	1790.658	7.473
11-10 P(28)	1771.092	29.982
12-11 P(22)	1771.951	9.526
13-12 P(16)	1771.327	150.691
15-14 P(25)	1685.159	80.242
16-15 P(19)	1684.835	961.812
17-16 P(13)	1683.016	56.716
17-16 P(25)	1636.165	20.979
18-17 P(19)	1635.589	404.659
19-18 P(13)	1633.519	2.199
17-16 P(26)	1632.054	0.865
18-17 P(20)	1631.703	0.767
19-18 P(14)	1629.863	0.726

coefficients are mean values of the absorption coefficients at the individual lines, weighted by their relative intensities. The latter depend on the actual angle of the grating, the cavity length, the discharge current etc., and are not exactly reproducible. Therefore, the water vapor spectrum that has to be subtracted from the PA spectrum of the air sample, has to be determined for each measurement independently. This is achieved by an experimental setup in which two identical PA cells are operated in a parallel arrangement as shown below in Fig. 3.

1.2. Desired Spectrophone Properties

Based on above considerations, an optimum cell to be used in CO-laser PAS should fulfill the following requirements:

i) the sensitivity should be as high as possible in order to decrease the influence of the microphone noise at low laser powers,

ii) the design should permit to operate the cell at an acoustic resonance and to place Brewster windows at the pressure nodes of this resonance in order to minimize the synchronous background signal due to the window heating effect,

iii) the resonance frequency should lie between 400 and 1500 Hz where the noise of the microphone in use is minimal,

iv) the parallel operation of two identical cells requires the tuning of the resonance frequency of one of the cells,

v) the quality-factor Q of the acoustic resonance should not exceed 100 in order to decrease the influence of small deviations from the resonance frequency.

Conventional PA cells [7–10], e.g. a cylindrical cell operated at a radial resonance with Brewster windows mounted at the pressure nodes of the first radial mode as presented by Gerlach and Amer [7], do not fulfill all these requirements. Therefore, a new type of cell

operating at longitudinal acoustic modes or at Helmholtz resonances had to be developed.

In the following sections a general procedure is presented that permits the calculation of acoustic properties of one-dimensional PA cells. Based on these calculations various types of cells have been studied and a design was found which best fulfills all the requirements listed above.

2. Theory

2.1. Analogue Acoustic Impedances

The acoustic behavior of a tube can be represented by an electric equivalent model as long as the wavelength of the sound wave is much larger than the cross-sectional dimensions of the tube [11–13]. The sound pressure amplitude p is the acoustic analogue of the voltage U, and the total flux $Y=Sv$ of the fluid with velocity v through the cross section S of the tube is the acoustic analogue of the electric current I. Further, a heat source in the acoustic arrangement, such as the laser energy absorbed by the molecules in the gas, is the acoustic equivalent of an electric current source I^0. For a laser power amplitude W_L at the circular modulation frequency ω and an absorption coefficient α_L of the fluid at the laser wavelength λ, the analogue of the electric current source per unit length of the tube is given by [12]:

$$dI^0/dx=(\gamma-1)W_L\alpha_L/(\varrho c^2) \tag{1}$$

where $\gamma=C_p/C_v$ is the ratio of specific heats at constant pressure and volume, ϱ is the density and c is the velocity of sound. The analogue acoustic inductance L_a, the capacitance C_a and the resistance R_a of a tube with cross section S, perimeter D and length l are defined as follows [12]:

$$L_a=\varrho l/S, \tag{2}$$

$$C_a=lS/(\varrho c^2), \tag{3}$$

$$R_a=\varrho lD/(2S^2)\omega[d_v+(\gamma-1)d_h], \tag{4}$$

where

$$d_h=(2\mu/(\varrho\omega))^{1/2}=0.21(\omega/2\pi)^{-1/2}\ \text{cm Hz}^{1/2}, \tag{5}$$

$$d_v=(2K/(\varrho\omega C_p))^{1/2}=0.25(\omega/2\pi)^{-1/2}\ \text{cm Hz}^{1/2}, \tag{6}$$

d_h and d_v are the thicknesses of the boundary layers of the thermal and shear modes, respectively, μ is the viscosity, and K the heat conductivity. The numerical data in (5, 6) are valid for air at standard conditions. According to (4–6) the acoustic resistance is proportional to $\omega^{1/2}$ and not frequency-independent as the electrical resistance.

Equations (5, 6) are valid only if d_h and d_v are much smaller than the cross-sectional dimensions of the tube. This condition yields a lower frequency limit, while the upper frequency limit is reached when the wavelength of sound is comparable to the cross-sectional dimensions of the tube.

2.2. Approximation with Discrete Impedances

If the source of sound is well located, discrete analogue acoustic impedances are well suited for calculating the acoustic behavior of transmission lines [11–13]. For the case of a long spectrophone where the generation of sound is distributed over the whole length of the cell, a model using continuous impedances and current sources has to be applied. This will be discussed in Sects. 2.3 and 4.

In order to derive some general relations, it is instructive to study the behavior of acoustic analogue circuits containing only discrete impedances and sources. If a long tube is divided into two parts, it can be considered as a Helmholtz resonator. As an example, the analogue circuit representing a discrete source at one end of a tube is shown in Fig. 2. The following relations are obtained for the signal amplitude U, the resonance frequency ω_0 and the quality factor Q:

$$U=\frac{1}{i\omega C_a}\,\frac{\omega_0^2-2\omega^2+2i\omega\omega_0/Q}{\omega_0^2-\omega^2+i\omega\omega_0/Q}\,I^0, \tag{7}$$

$$\omega_0=2(L_aC_a)^{-1/2}=2c/l, \tag{8}$$

$$Q=\omega_0L_a/R_a=2S/(D[d_v+(\gamma-1)d_h]). \tag{9}$$

Equations (1, 3, and 7) permit the calculation of the cell constant $F=p/(\alpha_LW_L)$ which relates the pressure amplitude p with the absorbed laser power. For a PA cell with a volume V and an absorption pathlength l that is operated at a resonant mode with the resonance frequency ω_0 and the quality factor Q, one obtains

$$F(\omega_0)=(\gamma-1)lQG/(i\omega_0V). \tag{10}$$

G is a geometrical factor of the order of 1 which cannot be derived from this simplified model.

A qualitative behavior for ω_0 and Q can also be derived from simple geometrical considerations. The tube length l has to be a multiple of half the wavelength of an acoustic resonant mode. The quality factor Q is given by the ratio of the energy stored in a specific mode divided by the energy losses per cycle [8, 9, 11]. The losses are proportional to the cell surface A and to the thicknesses $d_h\approx d_v=d$ of the boundary layers, while the total energy is proportional to the cell volume. Therefore, the following relations can be derived for a cylindrical spectrophone of radius r and length $l\gg r$ operated at a longitudinal mode

$$\omega_0\propto l^{-1}, \tag{11}$$

$$Q(\omega_0)\propto V/(Ad)\propto rl^{1/2}/(r+l)\simeq r/l^{1/2}, \tag{12}$$

$$F(\omega_0)\propto l^{1/2}/r. \tag{13}$$

If the spectrophone is operated at a radial resonance, the equivalent relations are

$$\omega_0 \propto r^{-1}, \tag{14}$$

$$Q(\omega_0) \propto V/(Ad) \propto l r^{1/2}/(r+l) \simeq r^{1/2}, \tag{15}$$

$$F(\omega_0) \propto l/[r^{1/2}(r+l)] \simeq r^{-1/2}. \tag{16}$$

These equations show that the product $Q(\omega_0)F(\omega_0)$ is nearly independent of the cell dimensions for any kind of resonant PA cell. The operation of the cell at a longitudinal mode is more advantageous because it permits to optimize the resonance frequency and the Q-factor independently, which is not possible for the case of a radial resonance.

2.3. Sound Generation and Propagation in a Long Tube

The laser generation and the propagation of an acoustic wave in a tube of length l can be calculated by considering an infinitesimal element of length Δl within the tube. The acoustic behavior can be represented by an analogue electric circuit, as shown in Fig. 2. The discrete values for the impedances and the current source are replaced by the corresponding infinitesimal values. U and I are represented by functions of the position x within the tube. For a harmonic sound generation, the resulting differential equations for $U(x)$ and $I(x)$ representing the pressure amplitude and the total flux of fluid, respectively, are

$$dU/dx = -Z_1 I/l, \tag{17}$$

$$dI/dx = -1/Z_2 U/l + dI^0/dx, \tag{18}$$

with

$$Z_1 = i\omega L_a + R_a \quad \text{and} \quad 1/Z_2 = i\omega C_a. \tag{19}$$

For the case of a homogeneously distributed current source $dI^0/dx \equiv \overline{I^0}/l$, the solutions of (17, 18) are given by

$$I(x) = A e^{\beta x/l} + B e^{-\beta x/l}, \tag{20}$$

$$U(x) = Z_2[\overline{I^0} - \beta(A e^{\beta x/l} - B e^{-\beta x/l})], \tag{21}$$

with

$$\beta = (Z_1/Z_2)^{1/2}. \tag{22}$$

The coefficients $A = A(\omega)$ and $B = B(\omega)$ are integration constants to be determined by the boundary conditions.

The total pressure amplitude $p(x)$ at any location x within the tube can be separated into a term independent of x caused by the heating of the gas and into two damped waves propagating in positive and negative x-direction. The frequency-dependent coefficients A and B in (21), which permit the calculation of the pressure amplitude anywhere in the tube, depend on the acoustic impedances at the tube ends. The tube as a whole is the acoustic analogue of an electrical four-terminal containing a current source.

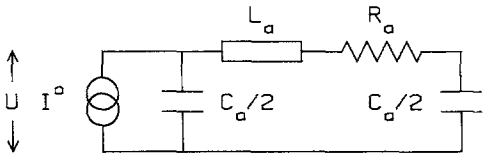

Fig. 2. Analogous electric circuit for a long photoacoustic cell considered as a Helmholtz resonator

2.4. Matrix Formalism

A one-dimensional PA cell can be divided into a finite number N of tube elements with length l_i, perimeter D_i, cross section S_i, etc. Each element i ($i = 1 \ldots N$) represents a four-terminal in the analogue electric circuit. The boundary conditions

$$I_i(x_i = 0) = I_{i-1}(l_{i-1}) \quad \text{and} \quad U_i(x_i = 0) = U_{i-1}(l_{i-1}) \tag{23}$$

for the current I and the voltage U determine a relation between the coefficients A and B of adjacent four-terminals. On the basis of (20, 21) this relation can be transformed into an inhomogeneous matrix equation

$$\begin{bmatrix} A_i \\ B_i \end{bmatrix} = \begin{bmatrix} M_{i,11} & M_{i,12} \\ M_{i,21} & M_{i,22} \end{bmatrix} \begin{bmatrix} A_{i-1} \\ B_{i-1} \end{bmatrix} + \begin{bmatrix} V_{i,1} \\ V_{i,2} \end{bmatrix}, \tag{24}$$

where the matrix elements $M_{i,rs}$ ($r, s = 1, 2$) contain the impedances of adjacent elements whereas the vector elements $V_{i,r}$ contain the sources.

By iteration one obtains an analogue matrix equation between (A_1, B_1) and (A_N, B_N), correlating the coefficients of the first and the last element. The boundary conditions at the beginning and at the end of the cell-configuration yield two more equations. If the cell windows are represented by the impedances $Z_{w,0}$ and $Z_{w,N}$ (usually almost infinite), and the heat generated at the windows by the current sources $I_{w,0}$ and $I_{w,N}$, one obtains:

$$U_1(0) = Z_{w,0} \cdot [I_{w,0} - I_1(0)], \tag{25}$$

$$U_N(l_N) = Z_{w,N} \cdot [I_{w,N} + I_N(l_N)]. \tag{26}$$

With the aid of (20, 21) these equations can be transformed into equations relating A_1 with B_1 and A_N with B_N. This permits the calculation of A_1 and B_1. The matrix equation (24) enables to determine the coefficients A_i and B_i of the remaining elements by iteration.

The influence of small volumes like gas inlets etc. can be taken into account by placing additional four-terminals containing the discrete impedances corresponding to those volumes.

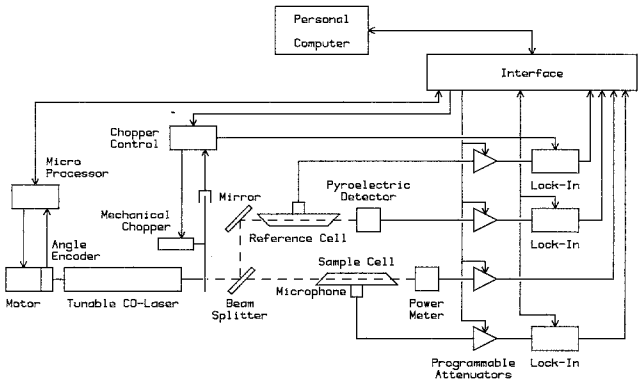

Fig. 3. Experimental setup for CO-laser PA measurements with reference cell

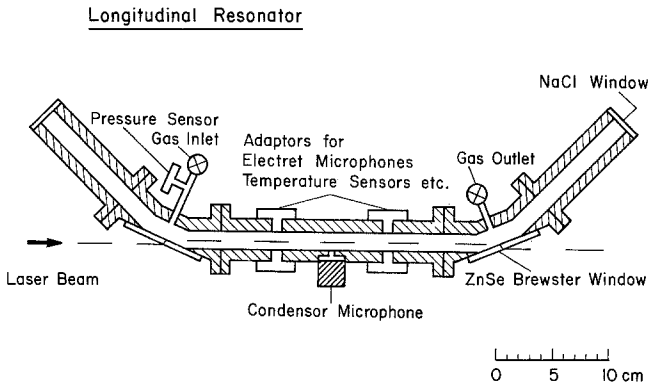

Fig. 4. Top view of the longitudinal resonant spectrophone. The ZnSe Brewster windows and the gas in- and outlet are mounted at the pressure nodes of the second longitudinal mode of the cell

3. Experimental

The experimental setup for PAS with our CO laser (Edinburgh-Instruments Type PL3) is shown in Fig. 3. Two identical PA cells are operated in a parallel arrangement. The first cell contains the air sample under study while the reference cell is filled with water vapor diluted in a buffer gas (N_2 or synthetic air consisting of 80% N_2 and 20% O_2). A 70% transmission ZnSe beamsplitter is used to divide the *P*-polarized CO laser beam into two paths of identical length, providing the same spectral content of the beam in the two cells. The laser beam is modulated by a mechanical chopper and the PA signals are detected with condenser microphones (Brüel & Kjaer, Type 4179 and 4144). A personal computer (IBM, PC AT 03) is used to control the experiment with the aid of a data acquisition and control workstation (Keithley Instruments, System 570). Gain programmable attenuators are used to adapt the microphone signals to the ranges of the lock-in amplifiers (Ithaco, Dynatrac 393). The grating is positioned by a microprocessor-controlled motor (Oriel, motor-mike).

4. Results and Discussion

According to (12, 13) a long and narrow cell with a low *Q*-factor best fulfills the requirement of high sensitivity. The maximum length is restricted by the minimum frequency at which the cell should be operated or by the maximum absorption coefficient α_{max} that should be detected ($l \ll 1/\alpha_{max}$). The minimum possible diameter is fixed by the beam diameter or by the volume-to-surface ratio in order to minimize adsorption and desorption at the cell walls. On the other hand, a high quality factor *Q* is demanded in order to decrease the background signal caused by window heating. The optimum cell that best fulfills all the requirements is shown in Fig. 4. It has briefly been discussed in [14]. This novel cell geometry is obtained from the condition that the cell should be operated at a longitudinal mode with Brewster windows mounted at the pressure nodes.

We have chosen a cell with a total length *l* of 60 cm and a diameter 2*r* of 1.5 cm, operating at the second longitudinal mode. The absorption path length is 30 cm, the beam enters and exits the cell through ZnSe Brewster windows. Since the laser is not 100% *P*-polarized, a NaCl window, through which the residual part of the laser beam that is reflected at the second Brewster window can leave the cell, is mounted at the end. One of the two identical cells used in our experiment is equipped with a movable piston mounted at the front. This permits a fine tuning of the resonance frequency over a range of 20 Hz. At ambient conditions the measured resonance frequency ν_0 for an air sample containing 10 mb H_2O vapor (52% rH) is 555 Hz, the quality factor *Q* is 43 and the cell constant *F* is 1640 Pa cm/W. The calculated data for dry air are 554.9 Hz, 52 and 1990 Pa cm/W, respectively.

Figure 5 shows the dependence of the cell constant on frequency and position calculated with the matrix formalism. One would expect by symmetry considerations that only the even modes 2, 6, 10 etc. are excited by laser light absorption in the gas, while the absorption of laser light at the windows should activate only the remaining modes. Since a pressure gauge is attached at the gas inlet pipe, the cell symmetry is slightly broken and as a consequence odd modes are activated in addition to the even modes 2, 6, 10 etc. The same is valid for the even modes 4, 8, 12 etc. which are outside the frequency range plotted in Fig. 5. The asymmetric mode observed at a resonance frequency of 380 Hz is due to a Helmholtz resonance between the cell volume of 108 cm^3 and the pressure gauge volume of 3.1 cm^3.

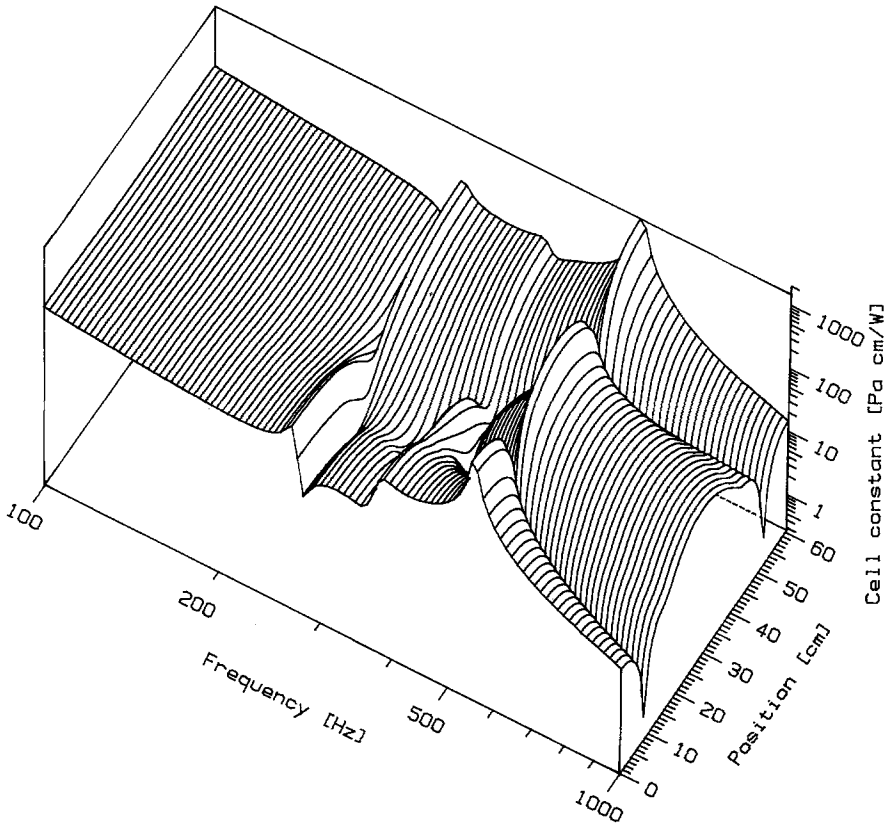

Fig. 5. Calculated frequency dependence of the cell constant along the axis of the longitudinal spectrophone. The mode at 380 Hz represents a Helmholtz resonance between the volumes of the cell and of the pressure sensor

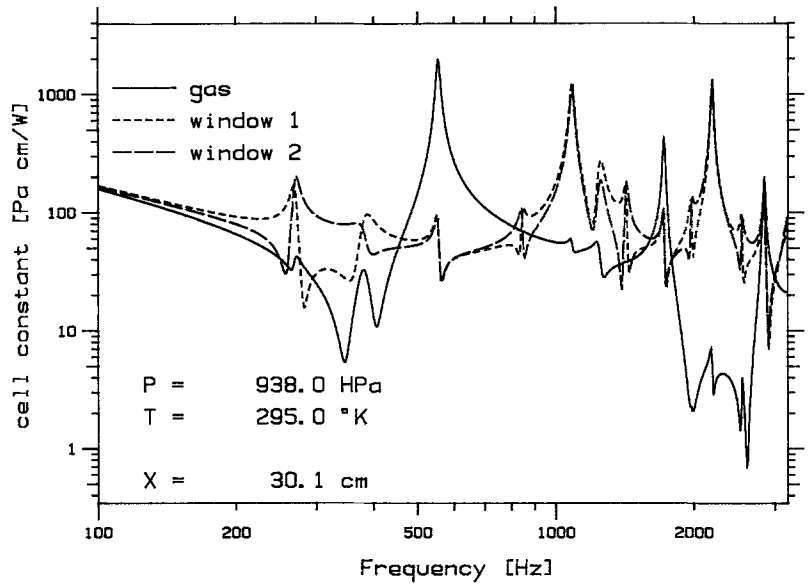

Fig. 6. Calculated frequency profiles of the PA signal at the center of the spectrophone ($x = 30.1$ cm) by absorption of laser radiation in the gas and at the windows. Window 1 and 2 represent the Brewster windows at the gas outlet and inlet, respectively

Figure 6 shows the frequency dependence of the cell constant for a microphone positioned at the center of the cell. This corresponds to a position at a pressure maximum of the even longitudinal modes and at a pressure node of all odd modes. This further reduces the influence of the odd modes if the cell is operated at the second longitudinal mode. The solid line represents the case where the laser radiation is absorbed only by the gas, while the dashed lines correspond to the cases where the same energy is absorbed totally at either one of the Brewster windows. The advantage of mounting the windows at the pressure nodes is well demonstrated, the window heating signal is decreased by the Q factor.

The response of the cell has been measured between 30 and 3000 Hz. Since the sensitivity of the micro-

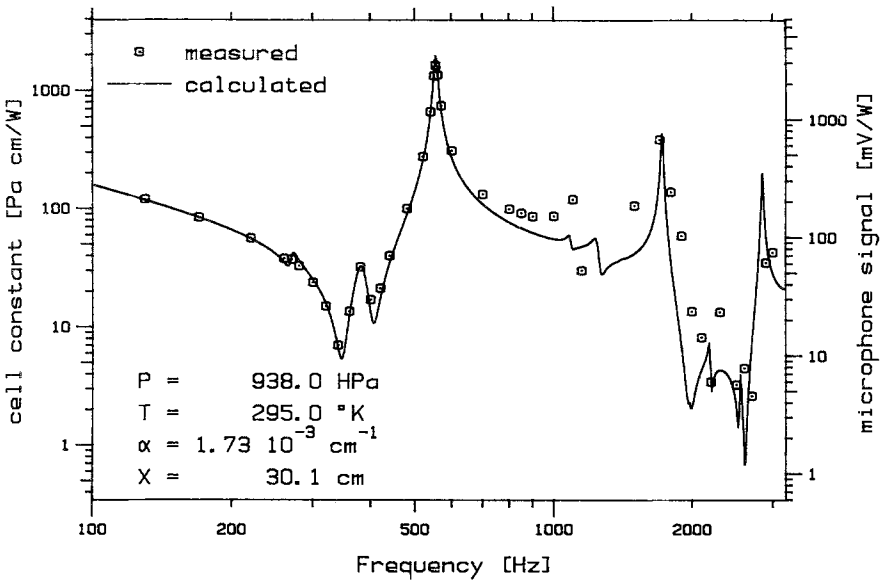

Fig. 7. Comparison between theoretical and experimental frequency profiles of the longitudinal resonator

phone is constant within this frequency range, the measured signal should be proportional to the cell constant F. In Fig. 7 the calculated frequency dependence of the cell constant is compared to the experimental data. The latter have been calculated from the absorption of the 6–5 $P(22)$ CO laser line in an air sample containing 10 mb water vapor. The agreement between theory and experiment is excellent for the "permitted" modes 2, 6, and 10 corresponding to 555, 1700, and 2800 Hz, respectively, while the predicted data for the "forbidden" modes 4 at 1100 Hz and 8 at 2200 Hz are too small. The deviations might be due to misalignment of the laser beam, window heating effects etc., or to incorrect theoretical approximations in considering the influence of the gas in- and outlet.

5. Conclusions

A theory based on infinitesimal analogue acoustic impedances and sources, combined with a matrix formalism for four-terminals, is used to calculate the acoustic properties of spectrophones. The excellent agreement between experimental and theoretical frequency profiles for various cell designs in a wide frequency range demonstrates the general applicability of the model to all kinds of one-dimensional PA cells.

Some general considerations imply that the sensitivity of a resonant spectrophone at the resonance frequency is inversely proportional to the Q factor of the resonance, while the coherent background signal caused by window heating is decreased by the Q factor, if the beam enters the cell at the pressure nodes of the resonance.

Based on these results a new type of resonant spectrophone with improved properties has been designed. The cell is operating at a longitudinal mode and the beam enters and exits the cell through Brewster windows mounted at the pressure nodes. The possibility of tuning the resonance frequency of the cell permits its use in a reference system.

The microphone noise-limited minimum detectable absorption coefficient is approximately $2 \cdot 10^{-10}$ cm^{-1} W Hz$^{1/2}$, while the synchronous background signal corresponds to an absorption coefficient of approximately $2 \cdot 10^{-8}$ cm^{-1}. Hence, microphone noise becomes dominant only at laser powers below 10 mW.

The new spectrophone has been designed for a CO-laser PA system for the monitoring of gaseous air pollutants in the presence of water vapor. The dual-beam system with a reference cell enables to determine the absorption caused by H_2O with an accuracy of $\simeq 1\%$. For a dried air sample a minimum detectable absorption coefficient α_{min} of approximately $5 \cdot 10^{-8}$ cm^{-1} is achieved. This permits the detection of trace gas concentrations with a resolution of approximately 10 ppbv.

Acknowledgements. This work was supported by the Swiss National Science Foundation, National Research Program 14, and by the ETH Zurich.

References

1. L.B. Kreuzer: The Physics of Signal Generation and Detection, in *Optoacoustic Spectroscopy and Detection*, ed. by Y.-H. Pao (Academic, New York 1977) pp. 1–25
2. V.P. Zharov, V.S. Letokhov: *Laser Optoacoustic Spectroscopy*, Springer Ser. Opt. Sci. **37** (Springer, Berlin, Heidelberg 1986)
3. M.W. Sigrist: J. Appl. Phys. **60**, R83 (1986)
4. L.B. Kreuzer, N.D. Kenyon, C.K.N. Patel: Science **177**, 347 (1972)

5. R.B. Dennis, H.A. Mackenzie, G. McClelland, F.H. Hamza: Opt. Laser Technol. **10**, 221 (1976)
6. L.S. Rothman, S.A. Clough, R.A. McClatchey, L.G. Young, D.E. Snider, A. Goldmann: "AFGL Atmospheric Absorption Line Parameters Compilation", Air Force Geophysics Laboratory, Hanscom AFB, Bedford, MA (1982)
7. R. Gerlach, N.M. Amer: Appl. Phys. **23**, 319 (1980)
8. R.H. Johnson, R. Gerlach, L.J. Thomas III, N.M. Amer: Appl. Opt. **21**, 81 (1982)
9. A. Karbach, P. Hess: J. Chem. Phys. **83**, 1075 (1985)
10. K. Veeken, N. Dam, J. Reuss: Infrared Phys. **25**, 683 (1985)
11. E. Kritchman, S. Shtrikman, M. Slatkine: J. Opt. Soc. Am. **68**, 1257 (1978)
12. P.M. Morse, K.U. Ingard: *Theoretical Acoustics* (McGraw-Hill, New York 1968) pp. 270–300, 322–325, 467–492
13. O. Nordhaus, J. Pelzl: Appl. Phys. **25**, 221 (1981)
14. St. Bernegger, P.L. Meyer, M.W. Sigrist: Digest 11th Int. Conf. on IR and mmWaves, Tirrenia-Pisa, I (1986), pp. 497–499